HUMAN MOVEMENT
2013, vol. 14 (4), 334–339

THE INFLUENCE OF DIFFERENT CARDAN SEQUENCES ON THREE-DIMENSIONAL CYCLING KINEMATICS

doi: 10.2478/humo-2013-0040

JONATHAN SINCLAIR [1] *, JACK HEBRON [1], HOWARD HURST [1], PAUL TAYLOR [2]
[1] Division of Sport Exercise and Nutritional Sciences, University of Central Lancashire, United Kingdom
[2] School of Psychology, University of Central Lancashire, United Kingdom

ABSTRACT
Purpose. Three-dimensional (3-D) kinematics are widely utilized to quantify movement in cycling analyses. Three-dimensional angular kinematics are obtained using the Euler/Cardan technique, however, Cardan angles are influenced by their ordered sequence and may affect the resultant angular parameters. An XYZ sequence of rotations is currently recommended, although this technique may not always be appropriate when coronal and transverse plane angles are quantified. This study aimed to determine the influence of the six available Cardan sequences on 3-D lower extremity kinematics during cycling. **Methods.** Kinematic information was obtained from twelve cyclists using an optoelectronic 3-D motion capture system operating at 250 Hz. Repeated measures ANOVAs were used to compare the kinematic parameters obtained using the six Cardan sequences, and intraclass correlations were employed to detect the presence of crosstalk across planes. **Results.** The results show that discrete kinematic parameters in the sagittal, coronal and transverse planes were significantly greater when using the YXZ and ZXY sequences. It was also observed that these sequences were associated with the strongest correlations from the sagittal plane and also exhibited evidence of gimbal lock. **Conclusions.** The results suggest that the accurate representation of 3-D kinematics during cycling should continue utilizing the XYZ sequence and avoid the use of the YXZ and ZXY sequences.

Key words: biomechanics, motion capture, Euler angles

Introduction

The use of three-dimensional (3-D) segmental kinematics is now widely utilized in cycling analyses [1]. Typically, 3-D angular kinematics are obtained using the Euler technique in which the position and orientation of a rigid segment axis is computed with respect to another [2]. When calculating a joint angle using the Euler method, there are two separate coordinate systems. In the case of a joint angle, each coordinate system belongs to a body segment as two adjoining segments represent a joint (e.g. shank relative to thigh represents a knee angle). One segment is delineated as the reference and the other segment moves relative to the reference segment allowing joint angles to be quantified. The quantification of Euler angles is achieved using an ordered sequence of rotations [2, 3].

An XYZ sequence of rotations in which X denotes sagittal plane, Y coronal plane and Z transverse plane motion is currently the most widely utilized and advocated sequence of rotations in 3-D kinematic analyses [4, 5]. This recommendation was developed around the notion that the first rotation be the one with the greatest angular displacement. Despite this recommendation, the dominance of sagittal plane rotations during most movements means that the first rotation can influence the coronal and transverse plane waveforms in a process known as "crosstalk" [5].

The lower extremity joints play a key role in the pedal stroke during cycling. The hip, knee and ankle rotations facilitate locomotion and transmit forces and rotational energy to the pedals [1]. However, between 42% and 65% of recreational cyclists may experience an overuse injury to the lower extremities as a result of cycling training [1]. The tri-planar nature of the pedal stroke has been linked to motions that may lead to maladaptive joint loading [6]. Therefore, given the potential clinical implications of the movement and its importance to the generation of rotational movement of the cranks, the correct interpretation of the movement is essential for future kinematics analyses.

A small number of analyses have inspected the effect of altering the Euler sequence of rotations on the resultant 3-D kinematic parameters [2, 3]. Schache et al. [2] investigated the influence of different Cardan sequences on lumbo-pelvic complex kinematics during running. They showed that differences between each of the Cardan angle sequences did not exceed 7.0° and 2.8° for the lumbar spine and pelvic motions, respectively. It was concluded that different Cardan angle sequences did not substantially affect 3-D lumbo-pelvic angular kinematic patterns during running. Sinclair et al. [3] examined the effects of altering the sequence of rotations on 3-D ankle joint kinematics during running. Their results showed that, in the transverse and coronal planes, peak angle and range of motion values using the

* Corresponding author.

YXZ and ZXY sequences were significantly greater than other sequences. Furthermore, utilization of YXZ and ZXY sequences was associated with the highest levels of planar crosstalk from the sagittal plane. However, these analyses examined the influence of altering the sequence of rotations in movements in which there is a relatively small amount of sagittal plane range of movement, and thus the potential for planar crosstalk from this plane was reduced.

Therefore, the most efficacious technique for the quantification of 3-D kinematics during movements such as cycling in which sagittal plane motion strongly predominates is not yet known. As such, the aim of this study was to examine the influence of the six available Cardan sequences on 3-D hip, knee and ankle joint kinematic parameters and planar crosstalk during the pedal cycle.

Material and methods

Twelve male participants volunteered to take part in this investigation. All were free from musculoskeletal pathology at the time of data collection. The mean characteristics of the participants were: age 22.61 ± 3.53 years, height 1.75 ± 0.09 m and body mass 75.29 ± 7.25 kg. Ethical approval for this project was obtained from the University of Central Lancashire's School of Sport Tourism and Outdoors' ethical committee.

All data collection was completed using a cycle ergometer (Ergomedic 874E, Monark Exercise, Sweden). Participants were required to cycle at a constant workload of 170 W, where a 2 kg load was placed in the ergometer's weight basket requiring them to maintain a cadence of 80 RPM throughout data collection. Saddle height was quantified using the LeMond [7] formula. Participants rode without cleats on flat pedals to minimize the effect of riding using unfamiliar pedal configurations.

Kinematic data were obtained using an eight camera optoelectronic motion capture system (Qualisys Medical AB, Sweden) using a capture frequency of 250 Hz. The calibrated anatomical systems technique [8] was used to quantify segmental kinematics. To delineate the anatomical frames of the right foot, shank and thigh, retroreflective markers were positioned unilaterally to the calcaneus, 1st and 5th metatarsal heads, medial and lateral malleoli, medial and lateral epicondyle of the femur, and greater trochanter. To describe the pelvic co-ordinate axes, additional markers were placed on the anterior (ASIS) and posterior (PSIS) superior iliac spines. Tracking clusters were also positioned on the shank and thigh segments. A static calibration trial was conducted during which the participant stood in the anatomical position in order for the positions of the anatomical markers to be referenced in relation to the tracking clusters (Fig. 1).

Data processing involved time normalization of the obtained kinematic curves to 100% of the pedal cycle. Movement trials were digitized using the included Qualisys Track Manager software and exported as C3D files.

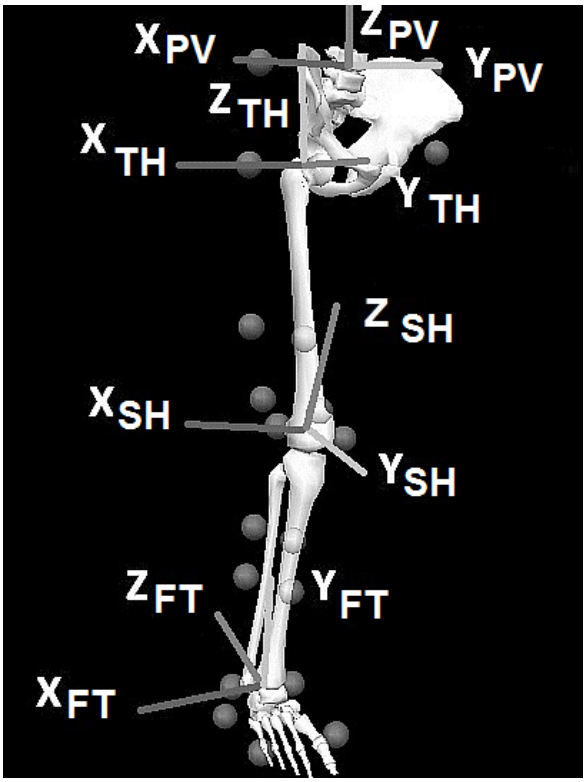

Figure 1. Pelvic, thigh, shank and foot segments, with segment co-ordinate system axes (P_{XYZ} – pelvis, SH_{XYZ} – shank; TH_{XYZ} – thigh, FT_{XYZ} – foot)

Kinematic parameters were quantified using Visual 3-D (C-Motion, USA) after marker data were smoothed using a low-pass Butterworth 4th order zero-lag filter at a cut-off frequency of 15Hz [9]. Three-dimensional kinematics of the hip, knee and ankle joints were calculated using XYZ, XZY, YXZ, YZX, ZXY and ZYX Cardan sequences referenced to co-ordinate systems about the proximal segment in accordance with previous recommendations [5]. The designations for rotations were: X – sagittal, Y – coronal and Z – transverse plane rotations. Discrete parameters of 1) peak angle during the pedal cycle, which could be either a maximum or minimum value, and 2) relative range of motion (ROM) from top dead centre-peak angle were extracted from each Cardan sequence from the full pedal cycle. All discrete variables used for statistical analysis were specific to each Cardan sequence.

Descriptive statistics including means and standard deviations were calculated for each Cardan sequence. Differences in these parameters as a function of the different Cardan sequences were examined using one-way repeated measures ANOVAs with a Bonferroni adjusted alpha criterion ($p \leq 0.003$) to control for type I error. Post-hoc pairwise comparisons also using a Bonferroni adjustment were utilized to examine significant main effects. Effect sizes were calculated using partial eta squared (η^2). Intra-class correlations (ICC) were utilized to compare between sagittal, coronal and transverse plane waveforms using the six different Cardan sequences.

Furthermore, sagittal plane angles from all three joints were also correlated with the associated coronal and transverse plane waveforms in order to identify evidence of planar crosstalk. All statistical procedures were conducted using SPSS ver. 20 (SPSS, USA).

Results

Figures 2–4 present the mean 3-D angular waveforms of the hip, knee and ankle joints during the pedal cycle. Tables 1–3 present relative ranges of motion and peak angles observed in all three planes of rotation as a function of Cardan sequence.

Hip

Comparisons between hip angles using the seven different methods revealed very strong correlations for the sagittal plane (ICC = 0.985). However, comparisons between the methods in the coronal (ICC = 0.170) and transverse (ICC = 0.101) planes revealed weak correlations between waveforms. When coronal and sagittal plane angles were correlated, very low correlations were observed when using the XYZ (ICC = 0.017), XZY (ICC = 0.017), YXZ (ICC = 0.09), YZX (ICC = 0.02), ZXY (ICC = 0.039) and ZYX (ICC = 0.024) techniques, indicating minimal extra-sagittal crosstalk. When transverse and sagittal plane angles were correlated, very low correlations were observed when using the XYZ (ICC = 0.033), XZY (ICC = 0.033), YXZ (ICC = 0.083), YZX (ICC = 0.038), ZXY (ICC = 0.033) and ZYX (ICC = 0.039) techniques, also indicating little crosstalk.

Knee

Comparisons between knee angles using the seven different methods revealed very strong correlations for the sagittal (ICC = 0.945) and transverse (ICC = 0.907) planes. However, comparisons between the methods in the coronal (ICC = 0.382) plane revealed weak correlations between waveforms. When coronal and sagittal plane angles were correlated, very low correlations were

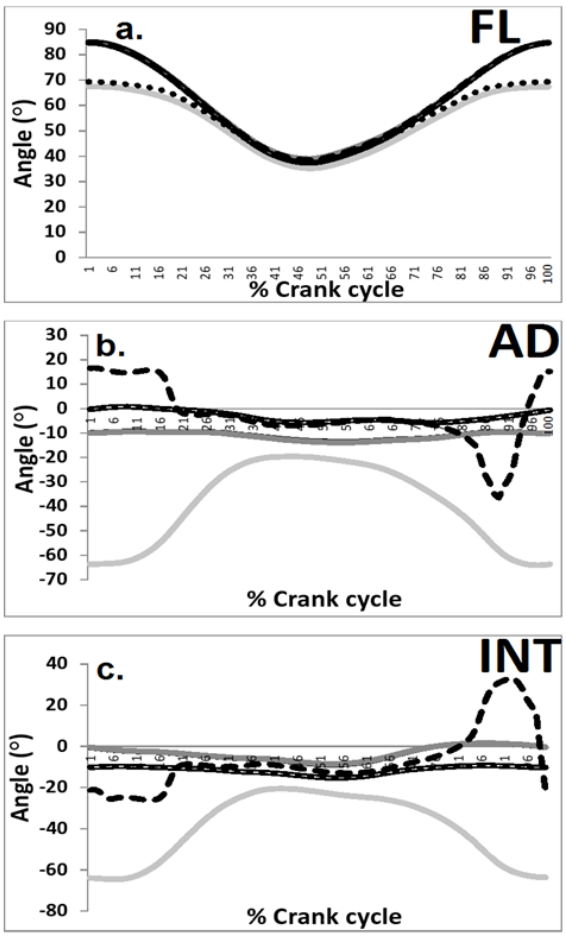

black line – XYZ, dark grey line – XZY, light grey line – YXZ, dotted line – YZX, dashed line – ZXY, black outline – ZYX

Figure 2. Hip joint kinematics as a function of Cardan sequence in the sagittal (a.), coronal (b.) and transverse (c.) planes during flexion (FL), adduction (AD) and internal rotation (INT)

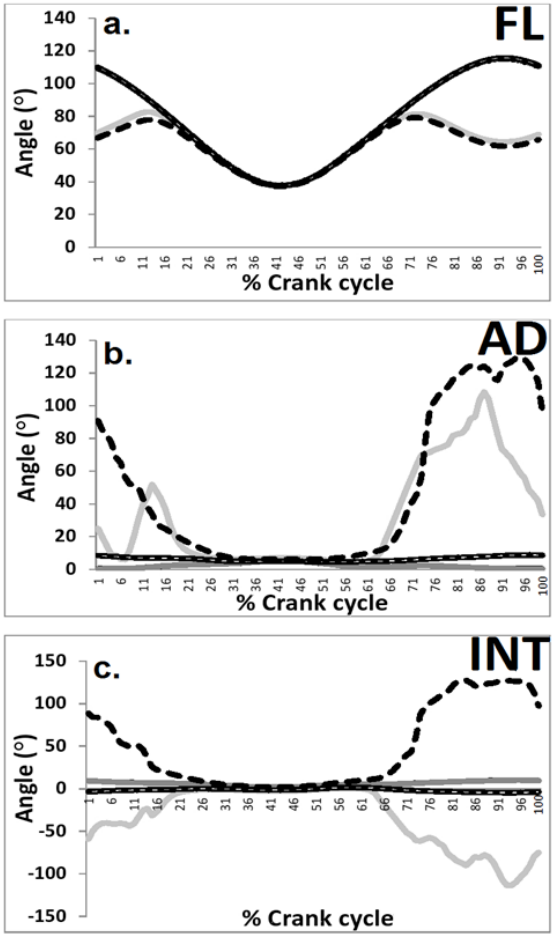

black line – XYZ, dark grey line – XZY, light grey line – YXZ, dotted line – YZX, dashed line – ZXY, black outline – ZYX

Figure 3. Knee joint kinematics as a function of Cardan sequence in the sagittal (a.), coronal (b.) and transverse (c.) planes during flexion (FL), adduction (AD) and internal rotation (INT)

Table 1. Hip joint kinematics of peak angle and relative range of motion (ROM) as a function of Cardan sequence

Hip	XYZ	XZY	YXZ	YZX	ZXY	ZYX	Statistical analysis	Post-hoc comparisons
Peak angle X (°)	36.97 ± 3.81	38.01 ± 5.86	35.33 ± 9.12	37.90 ± 6.13	37.93 ± 6.24	38.50 ± 5.80	$p = 0.298$, $\eta^2 = 0.10$	N/A
Peak angle Y (°)	–13.59 ± 3.81	–13.93 ± 4.21	–64.04 ± 8.99	–5.69 ± 4.51	–36.43 ± 7.38	–5.76 ± 4.33	$p = 0.0002$, $\eta^2 = 0.86$	*YXZ*, *ZXY* > XYZ, XZY, YZX, ZYX
Peak angle Z (°)	–8.85 ± 4.43	–8.56 ± 4.54	–64.58 ± 10.99	–15.20 ± 3.30	–33.02 ± 13.08	–15.31 ± 5.11	$p < 0.0001$, $\eta^2 = 0.89$	*YXZ*, *ZXY* > XYZ, XZY, YZX, ZYX
Relative ROM X (°)	47.03 ± 3.41	45.70 ± 4.11	32.20 ± 5.19	46.82 ± 3.80	31.31 ± 6.00	46.78 ± 4.19	$p < 0.002$, $\eta^2 = 0.42$	*YXZ*, *ZXY* > XYZ, XZY, YZX, ZYX
Relative ROM Y (°)	3.83 ± 5.11	3.99 ± 5.19	0.28 ± 3.71	5.21 ± 4.83	51.60 ± 4.09	5.41 ± 3.75	$p < 0.0009$, $\eta^2 = 0.67$	*ZXY* > XYZ, YXZ, XZY, YZX, ZYX
Relative ROM Z (°)	8.02 ± 3.22	8.11 ± 3.87	0.72 ± 4.31	5.10 ± 3.75	53.11 ± 13.22	4.71 ± 3.28	$p < 0.0008$, $\eta^2 = 0.71$	*ZXY* > XYZ, YXZ, XZY, YZX, ZYX

Table 2. Knee joint kinematics of peak angle and relative range of motion (ROM) as a function of Cardan sequence

Knee	XYZ	XZY	YXZ	YZX	ZXY	ZYX	Statistical analysis	Post-hoc comparisons
Peak angle X (°)	37.77 ± 10.11	37.88 ± 9.89	37.39 ± 11.10	37.91 ± 10.62	37.21 ± 9.87	37.64 ± 10.19	$p = 0.00008$, $\eta^2 = 0.96$	N/A
Peak angle Y (°)	5.17 ± 3.99	5.24 ± 4.22	108.51 ± 19.48	8.89 ± 4.36	129.62 ± 22.12	8.82 ± 4.11	$p = 0.00008$, $\eta^2 = 0.96$	*YXZ*, *ZXY* > XYZ, XZY, YZX, ZYX
Peak angle Z (°)	10.19 ± 3.81	10.15 ± 4.11	–113.81 ± 29.37	1.48 ± 5.65	127.59 ± 31.66	1.56 ± 5.86	$p = 0.00007$, $\eta^2 = 0.97$	*YXZ*, *ZXY* > XYZ, XZY, YZX, ZYX
Relative ROM X (°)	70.93 ± 16.98	71.32 ± 17.31	32.50 ± 25.39	70.49 ± 16.23	28.78 ± 19.91	72.34 ± 12.90	$p = 0.0003$, $\eta^2 = 0.56$	*YXZ*, *ZXY* > XYZ, XZY, YZX, ZYX
Relative ROM Y (°)	4.51 ± 3.11	4.87 ± 3.79	85.46 ± 21.85	0.51 ± 5.58	38.99 ± 7.72	0.66 ± 7.06	$p = 0.0001$, $\eta^2 = 0.88$	*YXZ*, *ZXY* > XYZ, XZY, YZX, ZYX
Relative ROM Z (°)	0.77 ± 3.10	0.68 ± 3.37	52.68 ± 15.92	5.00 ± 3.15	36.89 ± 10.17	5.05 ± 3.11	$p = 0.0008$, $\eta^2 = 0.76$	*YXZ*, *ZXY* > XYZ, XZY, YZX, ZYX

Table 3. Ankle joint kinematics of peak angle and relative range of motion (ROM) as a function of Cardan sequence

Ankle	XYZ	XZY	YXZ	YZX	ZXY	ZYX	Statistical analysis	Post-hoc comparisons
Peak angle X (°)	–3.95 ± 2.61	3.80 ± 2.75	–3.94 ± 2.63	–3.96 ± 3.05	–3.77 ± 2.14	3.78 ± 2.38	$p = 0.823$, $\eta^2 = 0.09$	N/A
Peak angle Y (°)	–0.47 ± 1.25	–0.48 ± 1.53	–0.49 ± 1.14	–0.75 ± 1.63	–0.79 ± 1.45	–0.74 ± 1.86	$p = 0.910$, $\eta^2 = 0.07$	N/A
Peak angle Z (°)	–5.46 ± 3.56	–5.53 ± 3.15	–6.05 ± 3.10	–5.87 ± 2.99	–5.89 ± 3.25	–5.87 ± 3.33	$p = 0.835$, $\eta^2 = 0.09$	N/A
ROM X (°)	16.70 ± 5.63	15.99 ± 6.11	16.54 ± 5.74	16.61 ± 5.58	16.08 ± 5.61	16.77 ± 5.55	$p = 0.620$, $\eta^2 = 0.21$	N/A
ROM Y (°)	2.98 ± 1.56	3.01 ± 2.00	2.99 ± 1.87	1.38 ± 2.43	1.33 ± 2.05	1.36 ± 2.22	$p = 0.423$, $\eta^2 = 0.29$	N/A
ROM Z (°)	4.20 ± 3.33	4.25 ± 3.55	5.10 ± 3.01	4.89 ± 3.26	5.03 ± 2.89	5.01 ± 3.09	$p = 0.590$, $\eta^2 = 0.18$	N/A

observed when using the XYZ (ICC = 0.022), XZY (ICC = 0.021), YZX (ICC = 0.025) and ZYX (ICC = 0.024) techniques, indicating minimal extra-sagittal crosstalk. However, when the YXZ (ICC= 0.350), ZXY (ICC = 0.364) sequences were utilized there was evidence of crosstalk. When transverse and sagittal plane angles were correlated, very low correlations were observed when using the XYZ (ICC = 0.043), XZY (ICC = 0.041), YZX (ICC = 0.021) and ZYX (ICC = 0.022) techniques, indicating minimal extra-sagittal crosstalk. However, when the YXZ (ICC = 0.100), ZXY (ICC = 0.374) sequences were utilized there was evidence of crosstalk.

Ankle

Comparisons between ankle angles using the seven different methods revealed very strong correlations for the sagittal (ICC = 0.999), coronal (ICC = 0.953) and transverse (ICC = 0.998) planes. When coronal and sagittal plane angles were correlated, very low correlations were observed when using the XYZ (ICC = 0.035), XZY (ICC = 0.038), YXZ (ICC = 0.095), YZX (ICC = 0.035), ZXY (ICC = 0.092) and ZYX (ICC = 0.039) techniques, indicating minimal extra-sagittal crosstalk. When transverse and sagittal plane angles were correlated, very low correlations were observed when using the XYZ (ICC = 0.045), XZY (ICC = 0.040), YXZ (ICC = 0.085), YZX (ICC = 0.034), ZXY (ICC = 0.085) and ZYX (ICC = 0.048) techniques, indicating little crosstalk.

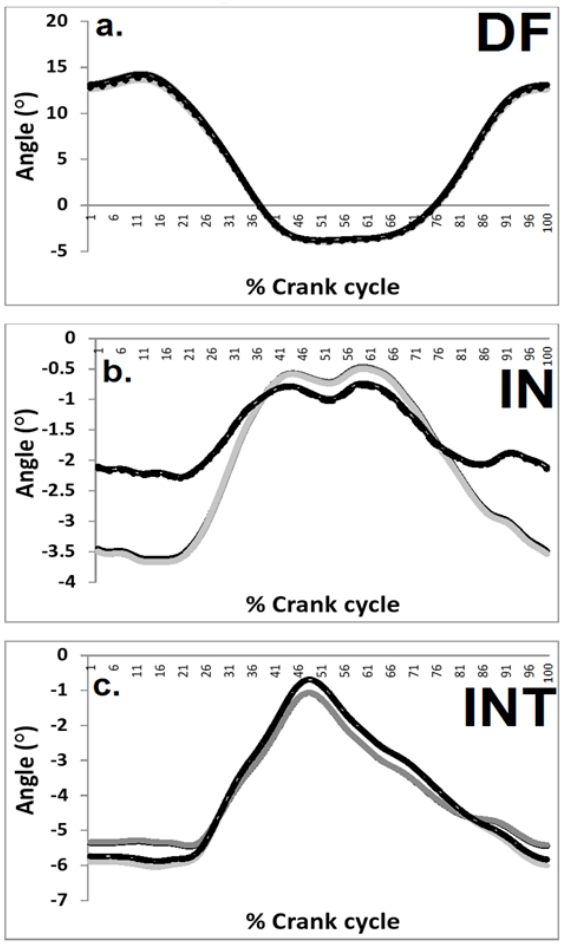

black line – XYZ, dark grey line – XZY, light grey line – YXZ, dotted line – YZX, dashed line – ZXY, black outline – ZYX

Figure 4. Ankle joint kinematics as a function of Cardan sequence in the sagittal (a.), coronal (b.) and transverse (c.) planes during dorsiflexion (DF), inversion (IN) and internal rotation (INT)

Discussion

The aim of the current investigation was to examine the influence of the six available Cardan sequences on 3-D hip, knee and ankle joint kinematic parameters and planar crosstalk during the pedal cycle. The current investigation represents the first to examine the influence of different Euler sequences of rotation on the 3-D kinematics of cycling.

The results of the current investigation show that altering the sequence of rotations in the sagittal plane significantly influences the obtained discrete kinematic parameters. This opposes the observations of Sinclair et al. [3] who found significant differences only in the coronal and transverse planes. They proposed, therefore, that altering the sequence of rotations does not significantly influence the resultant angular parameters when observing rotations in the sagittal plane. There are number of potential explanations for this observation. Sinclair et al. [3] examined only ankle joint kinematics, during which no significant alterations were observed, thus it is likely Sinclair et al. [3] were overly expansive in their conclusions having only considered ankle joint kinematics during gait. Secondly, the extent of sagittal plane movement during cycling is considerably greater than during normal running gait [10], thus the potential for alterations in the sagittal plane waveforms is accentuated.

In the coronal and transverse planes, significant main effects were observed in terms of peak angles and peak range of motion principally for the YXZ and ZXY sequences. The results indicate that with respect to the hip and knee joint profiles, these sequences were associated with extremely large values for peak angles. Furthermore, when coronal and transverse plane profiles were correlated with the sagittal plane, the strongest correlations were observed at the knee for the YXZ and ZXY sequences indicating that they cause the highest levels of planar crosstalk. The influence and magnitude of planar crosstalk on the resultant knee joint waveforms is such that they are anatomically impossible, highlighting the extent of the error when these sequences are utilized. This leads to the conclusion that these sequences cannot be utilized to accurately interpret knee joint function during cycling analyses.

It is interesting that despite the level of error that was apparently evident in the coronal and transverse plane profiles of the hip joint relatively low levels of planar crosstalk were observed. It is likely that this relates to

the lower sagittal plane angular range of movement observed at the hip when compared to the knee. However, observation of the hip joint kinematic waveforms in both the coronal and transverse planes suggests that gimbal lock is present in the YXZ and ZXY sequences. Gimbal lock transpires when the angular orientation approaches 90° and reflects a phenomenon whereby two rotational axes of an object are locked into a parallel configuration [11] causing the 3-D Euler rotation matrix to lose one degree of freedom. This corresponds with previous observations where gimbal lock was observed when the YXZ and ZXY sequences were utilized [11]. The fundamental implication of this finding is similar to those of the hip joint in that the waveform curves are unrealistic.

Of the three joints examined in the current investigation, the knee was the most susceptible to planar crosstalk. The magnitude of the ICC coefficients between sagittal and coronal/transverse plane profiles was much higher than those observed previously [2] at the ankle joint, indicating that additional crosstalk is present. Furthermore, in line with this observation there was very little crosstalk evident at the ankle joint and altering the Cardan sequence did not appear to influence the kinematic parameters. It is proposed that this relates firstly to the additional sagittal plane range of motion observed at knee joint during cycling when compared to typical gait profiles and secondly to the relatively minimal level of sagittal plane ankle motion during cycling. Therefore, the susceptibility of the non-sagittal profiles to crosstalk is increased, particularly when examining cycling movements in which the sagittal plane movement is dominant.

That the YXZ and ZXY were associated with the highest level of error is an interesting finding as placing X second in the order of rotations appears to be allied with the greatest degree of inaccuracy in determining angular rotations. The results of the current investigation provide further evidence for the existence of planar crosstalk and agree with the conclusions of Sinclair et al. [10], Lees et al. [11] and Kadaba et al. [12]. Observation of the angular profiles and statistical data suggests that it was stable across the range of joints in all planes of rotation and typically (although not universally) associated with the lowest degree of crosstalk. This suggests that there is little justification for altering the current consensus regarding utilization of the XYZ sequence to compute coronal and transverse plane kinematics in cycling.

Conclusions

These findings may have implications for researchers regarding the utilization of Cardan/Euler rotations as part of their 3-D kinematic data processing protocol during cycling analyses. The present study supports the continues utilization of the XYZ sequence for cycling analyses. In addition, the results suggest that the YXZ and ZXY sequences produce the greatest degree of error at the hip and knee joints, and thus the utilization of these sequences to quantify 3-D kinematics during cycling is discouraged.

References

1. Sinclair J., Theobald G., Atkins S., Weeks S.P., Hurst H.T., Biomechanical assessment of a professional road cyclist following recovery from severe injury: A case report. *J Sci Cycling*, 2013, 2 (1), 1–10.
2. Schache A.G., Wrigley T.V., Blanch P.D., Star R., Rath D.A., Bennell K.L., The effect of differing Cardan angle sequences on three dimensional lumbo-pelvic angular kinematics during running. *Med Eng Phys*, 2001, 23 (7), 493–501, doi: 10.1016/S1350-4533(01)00070-4.
3. Sinclair J., Taylor P.J., Edmundson C.J., Brooks D., Hobbs S.J., Influence of the helical and six available Cardan sequences on 3-D ankle joint kinematic parameters. *Sports Biomech*, 2012, 11 (3), 430–437, doi: 10.1080/14763141.2012.656762.
4. Wu G., Cavanagh P.R., ISB recommendations for standardization in the reporting of kinematic data. *J Biomech*, 1995, 28 (10), 1257–1261, doi: 10.1016/0021-9290(95)00017-C.
5. Richards J., Thewlis D., Anatomical models and markers sets. In: Richards J. (ed.), Biomechanics in clinic and research. Elseivier, Churchill Livingston 2008, 117–128.
6. Dannenberg A.L., Needle S., Mullady D., Kolodner K.B., Predictors of injury among 1638 riders in a recreational long-distance bicycle tour: Cycle across Maryland. *Am J Sports Med*, 1996, 24 (6), 747–753, doi: 10.1177/036354659602400608.
7. Lemond G., Gordis K., Greg Lemond's complete book of bicycling. Perigee Trade, New York 1987.
8. Cappozzo A., Catani F., Della C.U., Leardini A., Position and orientation in space of bones during movement: anatomical frame definition and determination. *Clin Biomech*, 1995, 10 (4), 171–178, doi: 10.1016/0268-0033(95)91394-T.
9. Winter D.A., Biomechanics and Motor Control of Human Movement. John Wiley & Sons, New York 1990.
10. Sinclair J., Richards J., Taylor P.J., Edmundson C.J., Brooks D., Hobbs S.J., Three-dimensional kinematic comparison of treadmill and overground running. *Sports Biomech*, 2013, 12 (3), 272–282, doi: 10.1080/14763141.2012.759614.
11. Lees A., Barton G., Robinson M., The influence of Cardan rotation sequence on angular orientation data for the lower limb in the soccer kick. *J Sport Sci*, 2010, 28 (4), 445–450, doi: 10.1080/02640410903540352.
12. Kadaba M.P., Ramakrishnan H.K., Wootten M.E., Measurement of lower extremity kinematics during level walking. *J Orthop Res*, 1990, 8 (3), 383–392, doi: 10.1002/jor.1100080310.

Paper received by the Editors: July 15, 2013
Paper accepted for publication: November 8, 2013

Correspondence address
Jonathan Sinclair
Division of Sport, Exercise and Nutritional Sciences
University of Central Lancashire
Preston, Lancashire
PR1 2HE, United Kingdom
e-mail: JKSinclair@uclan.ac.uk